



Optimal H-infinity PID Model Reference Controller Design for Roll Control of a Tail-Sitter VTOL UAV

Ali H. Mhmood  ^{a*}, Hazem I. Ali ^b

^a Control and Systems Engineering Department, University of Technology-Iraq, Baghdad, Iraq,
cse.19.16@grad.uotechnology.edu.iq

^b Control and Systems Engineering Department, University of Technology, Baghdad, Iraq,
60143@uotechnology.edu.iq

*Corresponding author.

Submitted: 14/10/2020

Accepted: 22/01/2021

Published: 25/04/2021

KEY WORDS

Black Hole
Optimization, H-infinity
Control, Model
Reference Control, PID
Controller, Robust
Control, Tail-Sitter
VTOL UAV System.

ABSTRACT

In this work, an optimal and robust controller based on consolidating the PID controller and H-infinity approach with the model reference control is proposed. The proposed controller is intended to accomplish a satisfactory transient response by including the reference model. A Tail-Sitter VTOL UAV system is used to show the effectiveness of the proposed controller. A dynamic model of the system is formulated using Euler method. To optimize the design procedure, the Black Hole Optimization (BHO) method is used as a new Calibration method. The deviation between the reference model output and system output will be minimized to obtain the required specifications. The results indicate that the proposed controller is very powerful in compensating the system parameters variations and in forcing the system output to asymptotically track the output of the reference model.

How to cite this article: A. H. Mhmood, and H. I. Ali, "Optimal H-infinity PID Model Reference Controller Design for Roll Control of a Tail-Sitter VTOL UAV," Engineering and Technology Journal, Vol. 39, Part A, No. 04, pp. 552-564, 2021.
DOI: <https://doi.org/10.30684/etj.v39i4A.1861>

This is an open access article under the CC BY 4.0 license <http://creativecommons.org/licenses/by/4.0>

1. INTRODUCTION

Unmanned Aerial Vehicles (UAVs) are aircraft equipped for flying without pilots. Recently, the study and advancement of UAVs have developed because they can be utilized in applications ranging from civilian to military applications. They have been generally used in aerial imagery, mapping, monitoring, policing fields, etc. Typically, UAVs are classified as conventional fixed-wing or hovering rotary-wing aircraft frames. From one point of view, traditional fixed-wing aircraft have established reliability, long flight time, and flight efficiency, but they cannot fly or hover at low speeds. On the other point of view, although hovering platforms have the operational flexibility of having the option to take-off vertically, hover, and land vertically, they typically have drawbacks in forwarding flight, such as low speed and helpless continuance [1].

The vertical takeoff and landing (VTOL) platform, which is combining a rotary-wing aircraft's maneuverability with the high-level flight efficiency of a fixed-wing aircraft, has recently attracted much attention. A VTOL aircraft have intrinsic focal points on account of its hovering capabilities and provide many advantages in contrast to quad-rotor aircraft, such as high energy autonomy. There are various ways to execute VTOL maneuvers such as tilting-rotor, tilting-wing, thrust-vectoring, tail-sitting, etc. The easiest way is tail-sitting since the VTOL maneuver does not require extra actuators. A simple mechanism is desirable for UAVs as weight savings are important for the VTOL maneuver and have a cost-saving advantage [2].

A tail-sitter, as shown in Figure 1, is the simplest type of VTOL UAV aircraft taking off and landing on its tail, then horizontally tilting for forwarding flight. This type does not require additional actuators. It does not need a runway for release and recovery compared to traditional designs, because it has far greater operational flexibility and can fly from any small free space [3].



Figure 1: A tail-sitter VTOL UAV Aircraft [4]

There have been many approaches to control a tail-sitter VTOL UAV system, including the PID regulator [4], the model predictive controller [5], sliding mode control [6], disturbance observer-based (DOB) controller using H_∞ synthesis [7], active disturbance rejection control (ADRC) for attitude controller [8], and nonlinear robust controller [9]. As per past studies, a tail-sitter VTOL aircraft exhibits a natural unstable behavior in vertical flight. Also, during hover mode, tail-sitters have complex flight dynamics due to system uncertainties and external disturbances. In [4], the PID controller has been used to control the tail-sitter VTOL aircraft. The conventional PID design procedure was based on a plant with constant parameters. However, the design of a feasible controller should involve the analysis of the robustness of the parameters uncertainty, stability, and performance.

Robust control is the study and design of control systems when perturbations (uncertainties and disturbances) exist. One of the popular and powerful approaches in robust control system design is the H-infinity control. H-infinity control is an efficient method to reject disturbance and noise of the control systems as well as to compensate for system uncertainties, but the H-infinity control design approach may not achieve the required transient response specification. Therefore, a suitable model reference can be implemented to achieve asymptotic tracking of prescribed limits, and its performance is used as a required response [10, 11].

Control engineers are leaning towards simple controllers like PIDs, but H-infinity PID control software has not been previously available. Therefore, PID controllers need to be tuned rather than optimized. After the year 2010, the PID controller can be used within the H-infinity procedure and the H-infinity PID controller can now be optimized [12].

This paper aims to design an optimal H-infinity PID model reference controller to stabilize the rolling position of a tail-sitter VTOL aircraft during hovering flight. The Black Hole Optimization (BHO) algorithm is used to optimize the design procedure of the proposed controller.

The objectives of the proposed controller are: compensating for plant uncertainties, rejecting the external disturbances and control system measurement noise, and providing the asymptotic tracking to make the actual system model asymptotically tracks the reference model.

The rest of this paper is divided into the following sections. Section 2 describes the process of the BHO algorithm. The system modeling of a tail-sitter VTOL aircraft is given in the third section. In section 4, the controller design is presented. Section 5 introduces the simulation results and discussions for applying the proposed controller to the system. Finally, the conclusion is given in section 6.

2. BLACK HOLE OPTIMIZATION (BHO) METHOD

The BHO is a powerful metaheuristic population-based optimization method inspired by the black hole phenomenon. Like other population-based algorithms, the BHO algorithm begins with an initial population of candidate solutions to an optimization problem and an objective function calculated for them. The definition of a black hole (BH) is an object in space with a huge fastened mass. Therefore, Neighborhood objects have no possibilities to get away from their gravitational force. Anything, even light particles, will fall into a BH and vanish from our universe. As this method is a population-based algorithm, an initial population of candidate solutions to a given problem is created and distributed randomly in the search space with an objective function computed for them. After that, the best candidate is chosen at each iteration to be the black hole, and the rest form the stars. The evolution of the population is achieved by moving all the candidates, in each iteration, towards the best candidate (the black hole) based on their current location and random number according to the following formula [13]:

$$x_i(t+1) = x_i(t) + rand \times (x_{BH} - x_i(t)), \quad i = 1, 2, \dots, N \quad (1)$$

where $x_i(t+1)$ and $x_i(t)$ are the locations of the i th star at the iterations $(t+1)$ and (t) , respectively, x_{BH} is the location of the black hole in the search space, $rand$ is a random number in the interval $[0,1]$ and N is the number of stars. Next, the black hole starts gulping the closest stars. When the stars enter within the range of BH (or the event horizon), they are sucked up and replaced by newly created random candidates in search space. In BHO algorithm, the event horizon radius is determined as follows [13]:

$$R = \frac{f_{BH}}{\sum_{i=1}^N f_i} \quad (2)$$

where f_{BH} is the fitness value of the black hole and f_i is the fitness value of the i th star. As a star moves towards the black hole, a location with a lower cost than the black hole may be reached. In such a situation, the black hole moves to the star's location and vice versa. Then, the BHO algorithm starts with a new black hole in the new location, and then stars move to that new location. Figure 2 illustrates just how well the BHO algorithm determines the optimized values. The Black Hole Optimization method has two major advantages. First, it has a simple structure, so it is easy to implement. Secondly, it is liberated from parameter tuning issues [13].

The BHO algorithm's functionality is to find the optimal parameters for the proposed controller and the performance weighting function. Firstly, specify the number of populations and the problem parameters, which are the parameters that require optimization. Then, specify the cost function representing the performance index to be minimized. The optimized parameters are determined continuously. Consequently, the best cost, on each iteration, is calculated. Finally, the number of iterations depends on whether an acceptable solution is reached or the maximum number of iterations is exceeded. After a while, all the best costs would become the same, this means that there are no other best solutions. At this point, the algorithm should be stopped [14].

3. TAIL SITTER VTOL AIRCRAFT SYSTEM MODEL

Modeling of a VTOL aircraft is described in this section. The first phase in a system controlling is to derive a mathematical model for it. The behavior of each of the system components can be extracted from fundamental physics. Figure 3 shows the VTOL aircraft schematic system during the flight mode. The VTOL aircraft is treated as a solid vehicle flying in aerospace and it is subjected to torques and forces applied to its frame depending on the type of object assumed. The VTOL aircraft needs high precision during landing and take-off maneuvers, so this flying object must be configured to control roll, pitch, and yaw actions in a restricted area [4].

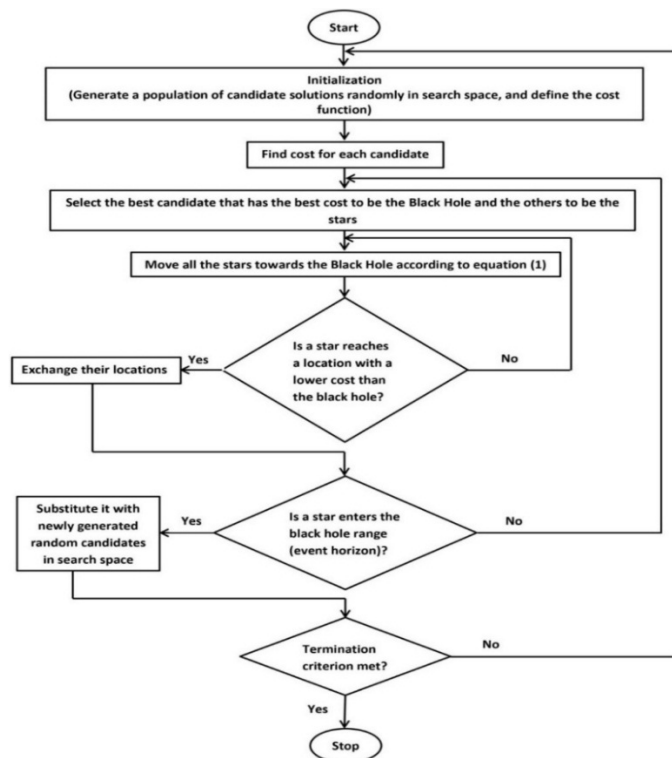


Figure 2: The BHO Algorithm flowchart

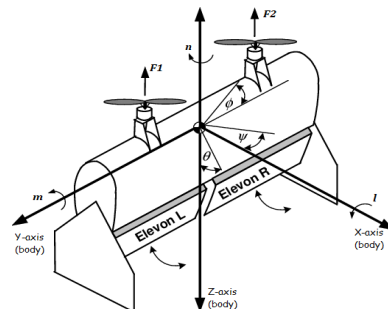


Figure 3: VTOL aircraft system schematic during the flight mode [6]

This paper aims to design an optimal H-infinity PID model reference controller capable of stabilizing the VTOL aircraft during hover flight, via controlling its rolling motion. The following assumptions are required for the modeling procedure:

Assumption 1 The aircraft is assumed to fly over a small local area on Earth that supports the use of the Flat-Earth model equations [15].

Assumption 2 The mass of the blades and elevons is neglected [1].

Assumption 3 For convenience, the vehicle's yaw and roll damping are not included in the model.

The model is derived from the analysis of the orientation of the VTOL aircraft in the inertial reference frame by the three Euler angles yaw, pitch, and roll. Euler angles are widely used in aerodynamic application fields. Based on Newton's motion equations, the set of behavior equations can be represented in terms of the following differential equations [4, 6].

$$\dot{P} = \frac{(J_y - J_z)QR}{J_x} + \frac{l}{J_x} \tag{3}$$

$$\dot{Q} = \frac{(J_z - J_x)RP}{J_y} + \frac{m}{J_y} \tag{4}$$

$$\dot{R} = \frac{(J_x - J_y)PQ}{J_z} + \frac{n}{J_z} \tag{5}$$

where [4]:

$\omega^b = [P \ Q \ R]^T$ represents the angular velocity for the body frame (X, Y, Z) , which is rotated to the north-east-down (NED) reference frame (x, y, z) .

$T = [l \ m \ n]^T$ is the torque applied to the center of mass of the VTOL aircraft in the body frame.

J_x, J_y and J_z are the diagonal elements of the diagonal inertia matrix J of the VTOL aircraft:

$$J = \begin{bmatrix} J_x & 0 & 0 \\ 0 & J_y & 0 \\ 0 & 0 & J_z \end{bmatrix} \tag{6}$$

To obtain the roll angle dynamics, only the roll subsystem is considered. In this situation, the pitch and yaw rates are assumed to be zero. The aircraft can be studied as a Planar Vertical Take-off and Landing (PVTOL) flight platform [16]. This means that pitch and yaw motion will be controlled by appropriate control laws in which $(Q = R = 0)$ is satisfied. Then, using equations (3), (4), and (5), the rotational dynamics of the roll angle can be described by [6]:

$$\ddot{\phi} = \frac{l}{J_x} \tag{7}$$

One can determine moments l as [6]:

$$l = Fd - C_l \dot{\phi} \tag{8}$$

where F is the difference in force between the right and the left rotors which represents the external thrust moment applied to the center of mass of the VTOL aircraft in the body frame (the control signal u). It can be expressed as [4]:

$$F = F_1 - F_2 = u \tag{9}$$

d refers to the distance of each rotor from the center of the mass of the VTOL aircraft and C_l is known as a roll damping derivative [4].

Substituting (8) in (7) gives [4]:

$$\ddot{\phi} = -\frac{C_l}{J_x} \dot{\phi} + \frac{d}{J_x} F \tag{10}$$

Letting $x = [x_1 \ x_2]^T = [\phi \ \dot{\phi}]^T \in \mathfrak{R}^2$ be the state vector of the system, $y = \phi = x_1 \in \mathfrak{R}$ be the controlled output and $u = F \in \mathfrak{R}$ be the control input. The system's standard equation description can be written as:

$$\dot{x}_1 = x_2, \dot{x}_2 = -\frac{C_l}{J_x} x_1 + \frac{d}{J_x} x_2 y = x_1 \tag{11}$$

Besides, the state equation can be written in matrix notation as:

$$\begin{bmatrix} \dot{x}_1 \\ \dot{x}_2 \end{bmatrix} = \begin{bmatrix} 0 & 1 \\ 0 & -\frac{C_l}{J_x} \end{bmatrix} \begin{bmatrix} x_1 \\ x_2 \end{bmatrix} + \begin{bmatrix} 0 \\ 1 \end{bmatrix} \left(\frac{d}{J_x}\right) u \tag{12}$$

The system dynamics become:

$$\dot{x} = Ax + B\Lambda u \tag{13}$$

where $B \in \mathbb{R}^{2 \times 1}$ is the known control matrix, while $A \in \mathbb{R}^{2 \times 2}$ and $\Lambda \in \mathbb{R}^{1 \times 1}$ are unknown constant matrices. Also, it is assumed that Λ is a diagonal matrix with positive entries and the pair $(A, B\Lambda)$ is controllable. The modeling errors are introduced as uncertainty in A and Λ matrices. The parameters d, C_l and J_x are considered to be uncertain with $\pm 10\%$ tolerances for each of them. The nominal values, upper, and lower bounds of the system parameters are listed in Table I.

Table I: List of system parameters [4]

Parameters	Lower bounds	Nominal values	Upper bounds
d	0.18 m	0.2 m	0.22 m
C_l	0.324	0.36	0.396
J_x	0.01296 kg.m ²	0.0144 kg.m ²	0.01584 kg.m ²

4. CONTROLLER DESIGN

In this section, the proposed controller is designed. The H-infinity control approach has been used to design an optimal PID controller for a tail-sitter VTOL aircraft system in such a way that the following requirements are met [17]:

- Robust stability and robust performance for different model parameter variations.
- Disturbance rejection and measurement noise attenuation.
- Low control effort.
- Low closed-loop bandwidth.
- The selected reference model specifications.

The performance analysis in H-infinity control is defined in terms of sensitivity function $S(s)$ and complementary sensitivity function $T(s)$ where [18]:

$$S(s) = \frac{1}{1+GK(s)} \tag{14}$$

$$T(s) = \frac{GK(s)}{1+GK(s)} \tag{15}$$

and $S(s) + T(s) = 1$.

The H-infinity control design has the flexibility to handle both structured and unstructured uncertainties. However, it is hard to work with structured uncertainty shapes. The solution is to replace these complicated structured uncertainty shapes with unstructured ones. Therefore, the unstructured multiplicative uncertainty model can be used to represent the plant with structured uncertainties [19]. Multiplicative perturbation model is relative or percentage uncertainty, where all that is assumed to be known about perturbation is that all right-hand poles (RHPs) of the real plant model $G_p(s)$ are entirely included in the nominal model $G(s)$ and they must have a finite known upper bound [18]. Figure 4 demonstrates the standard overall block diagram of the controlled system with system uncertainties and weighting functions. In this figure, $r \in \mathbb{R}$ represent the external command signal, $d \in \mathbb{R}$ is the external disturbance signal, $y_{ref} \in \mathbb{R}$ refer to the reference model output and $e_r(t) \in \mathbb{R}$ is called the tracking error, which is the difference between reference model output y_{ref} and the output of the actual system y . $W_p(s)$ represents the performance weighting function associated with performance requirements, which is used to convey specifications on the shape of the output sensitivity function $S(s)$, while $W_m(s)$ represents the multiplicative uncertainty weighting function calculated to cover ± 10 percent variance of the system parameters d, C_l and J_x .

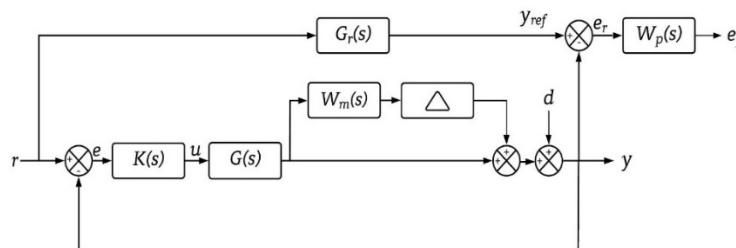


Figure 4: Block Diagram of the overall control system with weighting functions

The conditions of robust stability, in the situation of multiplicative uncertainty, are the control system with stabilizing controller $K(s)$ must be nominally stable (the controller stabilizes the nominal model $G(s)$) and [17]:

$$\|W_m T\|_\infty < 1 \quad (16)$$

The conditions of robust performance for a control system with multiplicative uncertainty are: the control system with stabilizing controller $K(s)$ must be nominally stable and $\mu < 1$, where [17]:

$$\mu = \|W_p S + W_m T\|_\infty \quad (17)$$

One of the essential phases of the H-infinity control approach is the choice of weighting functions for a particular design problem. After selecting the nominal model of the plant, the uncertainty weighting function is obtained by representing the plant uncertainties as a multiplicative uncertainty model according to the following equation [19]:

$$G_p(s) = G(s)(1 + \Delta_m(s)) \quad (18)$$

where $G_p(s)$ represents the actual plant model in terms of the uncertain system parameters, $G(s)$ is the plant nominal model in terms of nominal values of the uncertain parameters and $\Delta_m(s)$ is the multiplicative uncertainty model. From Eq. (18), the multiplicative uncertainty model can be written as [19]:

$$\Delta_m(s) = \frac{G_p(s) - G(s)}{G(s)} \quad (19)$$

Also, from [18]:

$$\Delta_m(s) = W_m(s)\tilde{\Delta}(s) \quad (20)$$

where $W_m(s)$ represents the uncertainty weighting function whose magnitude equals the upper bound of the multiplicative uncertainties $P_m(w)$:

$$|W_m(jw)| = P_m(w) \quad \forall w \quad (21)$$

and $|\tilde{\Delta}(jw)| \leq 1$. It is known that, from [20], the perturbed system geometrically can be thought of as a point in a ball that contains the nominal model and other members of the plant model family. The uncertainty weighting function is extracted from the upper bound of the multiplicative uncertainty model to cover all the points in a ball of uncertainty. Therefore, using Eq. (19), the uncertainty weighting function is determined by utilizing the curve fitting commands in MATLAB such that $|\tilde{\Delta}(jw)| \leq 1$ for all w [19]. The resulting uncertainty weight is:

$$W_m(s) = \frac{13.04s + 137.5}{s + 851.1} \quad (22)$$

The selected form of the performance weighting function [18]:

$$W_p(s) = \frac{\frac{1}{M_s} s + \omega_B}{s + \omega_B e_{ss}} \quad (23)$$

where ω_B is the minimal acceptable bandwidth to help in achieving adequate robustness, M_S is the maximum peak of the magnitude of sensitivity function $S(s)$. Typically, it is required that $M_S < 2$ to prevent high-frequency noise amplification and e_{ss} is the allowed steady-state error [18].

The PID controllers have always been the most popular in many industrial processes. The transfer function of PID controller is:

$$K(s) = \frac{U(s)}{E(s)} = K_p + \frac{K_i}{s} + K_d s \tag{24}$$

where K_p, K_i and K_d are the proportional, integral, and derivative PID gains (controller parameters) [21].

The H-infinity optimal control design approach may not meet the appropriate transient response specification. To overcome this scenario, an effective reference model may be applied and its output is used as the required response [22]. The specifications are mostly presented in terms of the standard quantity of rising time, settling time, overshoot, and steady-state error of time response. The step response of the standard second-order system is commonly used to describe the time-domain specifications as a reference model [23]. The reference model has important properties such as having to be stable, chosen so that the DC gain of the reference transfer function becomes unity, it is not part of the feedback design and therefore does not contribute to the transfer function of the closed-loop system [24]. The transfer function of the standard second-order system is given by:

$$G_r(s) = \frac{w_n^2}{s^2 + 2\xi w_n s + w_n^2} \tag{25}$$

where w_n is the natural frequency of the reference model and its value is chosen as 50 rad/s and ξ is the damping factor, which its value is chosen to be 0.85 . Their duty is to manage and prepare the desired specifications. Therefore, the proposed controller is an effective controller developed on the foundations of the H-infinity control strategy to achieve robustness functionality and incorporated with the model reference control technique to attain the desired transient response characteristics. The proposed scheme is shown in Figure 5.

The parameters to be optimized are the PID controller parameters (K_p, K_i and K_d) and the parameters of the performance weighting function (ω_B, M_S and e_{ss}). Some analyses were carried out to distinguish the optimal parameters of both the performance weighting function and the controller to maintain a satisfactory transient response with good robustness. Since the requirements for robustness are $\|W_p S\|_\infty < 1$ and $\|W_m T\|_\infty < 1$, it is desirable to impose the upper bounds of $1/|W_p|$ and $1/|W_m|$ on the magnitudes of S and T respectively. Instead of explicitly enforcing certain conditions, we may enforce a nearly identical condition [18]:

$$\|N\|_\infty < 1 \tag{26}$$

where $N = \begin{bmatrix} W_p S \\ W_m T \end{bmatrix}$.

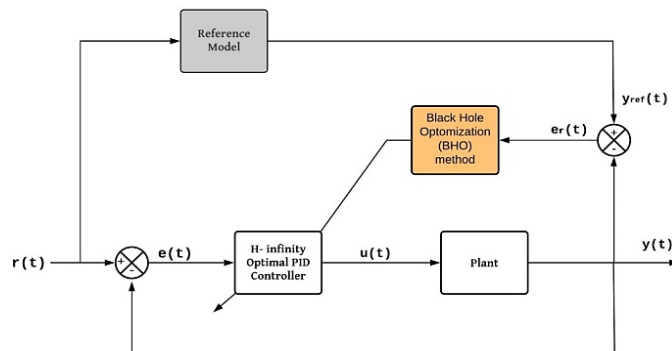


Figure 5: Block Diagram of the proposed Control System

As an outcome of these tests, it has been shown that the following cost function is more efficient and consistent to achieve the objectives of the proposed controller:

$$J(K_p, K_i, K_s, \omega_B, M_s, e_{ss}) = \int_{t_o}^{t_f} e_r(t)^2 dt + \|N\|_\infty \quad (27)$$

where t_o and t_f are the initial and final time, respectively. It is interesting to make the system output globally asymptotically tracks the output of the reference model for all system parameter variations in the presence of system uncertainties. During this tracking, the closed-loop system signals remain bounded. Therefore, for any bounded reference roll angle, the control input u must be applied in such a manner that the tracking error $e_r(t)$ globally asymptotically tends to be zero as $(t \rightarrow \infty)$ [24]:

$$\lim_{t \rightarrow \infty} |y_{ref} - y| = 0 \quad (28)$$

5. RESULTS AND DISCUSSION

This section presents the simulation and implementation of the optimal H-infinity PID model reference controller, which is introduced in the previous section, for a tail-sitter VTOL UAV aircraft system using the BHO algorithm. The results are presented with and without the proposed controller, which expressly illustrates the expected benefits of the proposed control strategy. The amplitude of the required angle applied within all simulation results in this paper is (30 degrees). Figure 6 shows the open-loop and closed-loop system time responses before applying the proposed controller. According to this figure, it is very noticeable that the development of the controller is crucial to regulate the system and perform an appropriate performance. The BHO algorithm is therefore used to obtain the optimal parameters of the proposed controller $K(s)$ and the performance weighting function $W_p(s)$. The optimization settings for BHO are given in Table II. Figure 7 indicates the cost function convergence rate of the BHO algorithm. It is shown that the convergence is fulfilled just after (150) iterations and the convergence minimization is established. The optimal parameters and their bounds are listed in Table III. Figure 8 shows the frequency response of nominal complementary sensitivity function $T(s)$ and nominal sensitivity function $S(s)$. Figure 9 shows the frequency response of $S(s)$ with the $W_p(s)$ inverse, while Figure 10 shows the frequency response of $T(s)$ with the inverse of the uncertainty weighting function $W_m(s)$. From the two figures mentioned earlier, it is noticed that the magnitudes of $S(s)$ and $T(s)$ for all frequencies are lower than the magnitudes of $W_p(s)^{-1}$ and $W_m(s)^{-1}$, respectively, indicating that robust performance and robust stability conditions have been met. The roll control signal behavior is expressed in Figure 11. Figure 12 shows the time response specifications of the controlled system using an H-infinity optimal PID model reference controller. The output of the system using the proposed controller tracked the output of the reference model. Furthermore, it is shown that the proposed controller is capable of achieving good robust performance. The transient response specifications obtained by the proposed controller are shown in Table IV in comparison with those achieved by the conventional PID controller developed in [4]. As a result, the proposed controller has been very successful in getting a satisfactory transient response identified by the model reference technique, the output of which was used as the desired system output response.

The time response of the uncertain controlled system is shown in Figure 13. It shows that the stability of the system in the presence of plant uncertainties with $\pm 10\%$ variations in the system parameters can be assured and the reference model being followed up. Figure 14 shows the controlled system's time response specifications for a different command signal, which is a train of steps 30, 45, 20, 60, and then back to 30 degrees, each step is applied for 1 second. The roll control signal of the aforementioned command signal is shown in Figure 15.

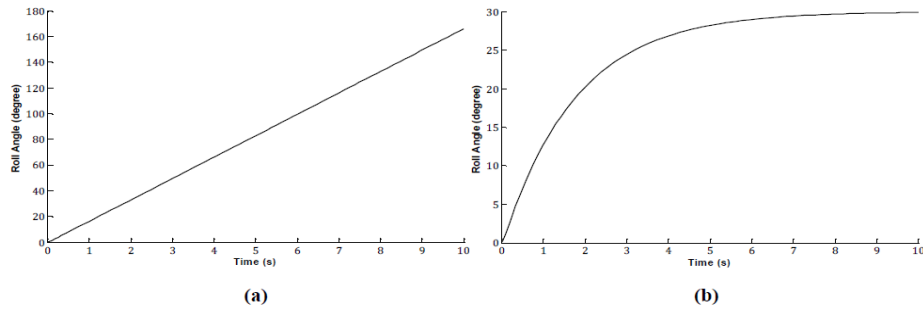


Figure 6: Time responses of the system before applying the controller (a) open-loop (b) closed-loop

Table II: List of BHO algorithm settings

Optimization settings	Number
Problem dimension (No. of parameters)	6
Size of population	50
No. of iterations	150
No. of runs	1

Table III: List of The optimal parameters and their bounds

Optimized parameters	Lower bound	Upper bound	Optimum value
K_p	0	200	100.7028
K_i	0	200	76.9314
K_d	0	100	3.1266
ω_B	0	0.1	0.0017
M_s	0	2	1.8974
e_{ss}	0	0.01	7.4×10^{-3}
Cost	-	-	0.8247

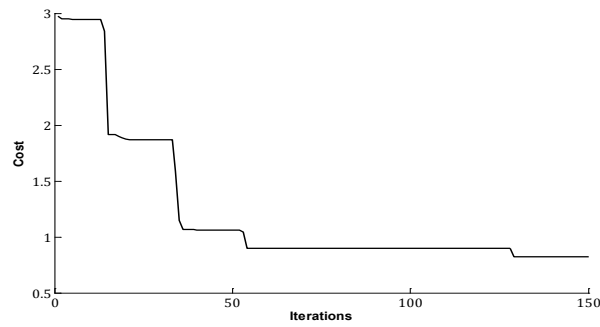


Figure 7: The cost function convergence

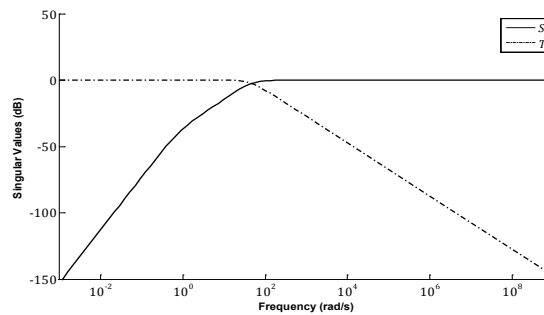


Figure 8: Frequency response characteristics of the nominal complementary sensitivity function ($T(s)$) and nominal sensitivity function ($S(s)$)

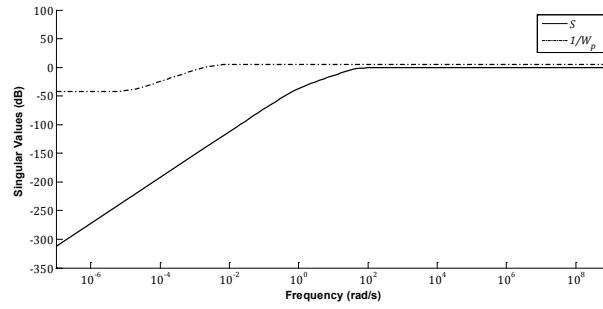


Figure 9: Frequency response characteristics of $(S(s))$ and (W_p^{-1})

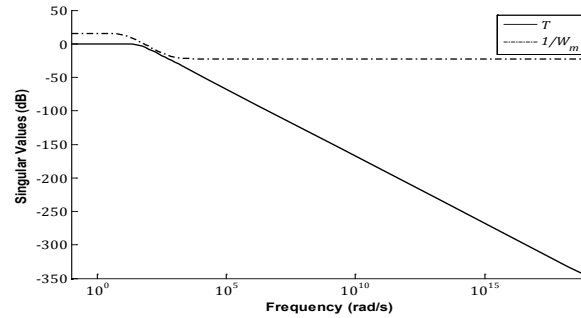


Figure 10: Frequency response characteristics of $(T(s))$ and (W_m^{-1})

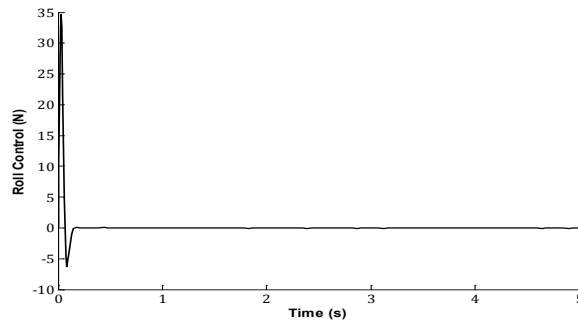


Figure 11: Behavior of roll control signal (thrust control)

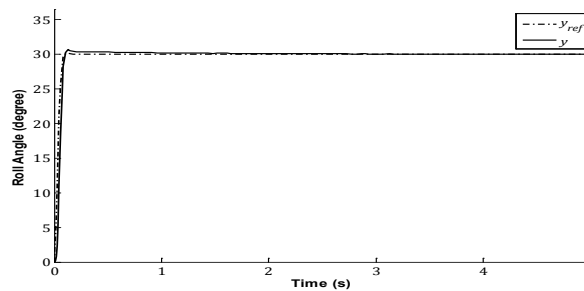


Figure 12: Time response characteristics of the controlled system

Table IV: The calculated transient response specifications compared to those resulting from [4]

Controller	transient response specifications	
	Rise time t_r (s)	Settling time t_s (s)
Conventional PID [4]	0.125	2.1
Proposed controller	0.0398	0.12

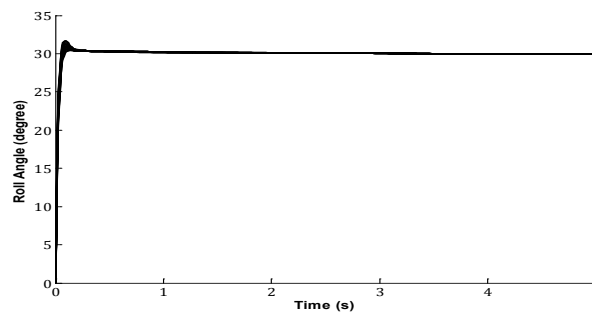


Figure 13: Time response characteristics of the controlled uncertain system

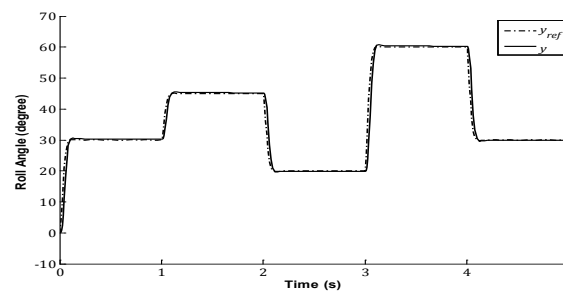


Figure 14: Time response characteristics of the controlled system for a train of steps

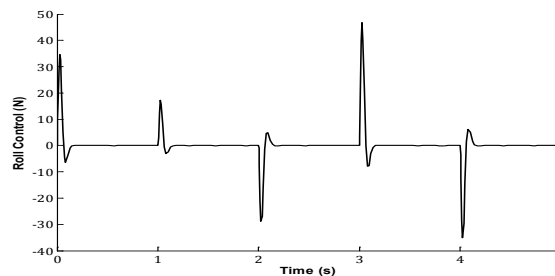


Figure 15: Behavior of roll control signal for a train of steps

6. CONCLUSION

In this paper, the model reference control strategy has been mixed with the H-infinity control approach and the PID controller to create a new robust control for roll control of a tail-sitter VTOL UAV system. In this methodology, the controller parameters have been optimized using the BHO algorithm such that the output of the controlled system asymptotically tracks the output of the reference model while all signals in the corresponding controlled system are bounded. The designed control method has established an asymptotic tracking of the desired reference model output for a given bounded command signal with compensating for the uncertainty of the system parameters. A variance in system parameters of ± 10 percent was taken into consideration. Finally, it was shown that the proposed control strategy could remedy the H-infinity controller's disadvantage in getting the required time response requirements, and could involve the robustness analysis for the PID controller.

References

- [1] K. C. Wong, J. A. Guerrero, D. Lara, R. Lozano, Attitude stabilization in hover flight of a mini tail-sitter UAV with variable pitch propeller, IEEE. Int. Conf. Intell. Robots. Syst., (2007) 2642–2647. <https://doi.10.1109/IROS.2007.4399278>
- [2] T. Matsumoto, K. Kita, R. Suzuki, A. Oosedo, K. Go, Y. Hoshino, A. Konno, M. Uchiyama, A hovering control strategy for a tail-sitter VTOL UAV that increases stability against large disturbance, IEEE. Int. Conf. Robot. Autom., (2010) 54–59. <http://doi.10.1109/ROBOT.2010.5509183>

- [3] O. Garcia, A. Sanchez, J. Escareno, R. Lozano, Tail-sitter UAV having one tilting rotor: Modeling, Control and Real-Time Experiments, IFAC, Proc. Volumes, 41(2008) 809-814. <http://doi.10.3182/20080706-5-KR-1001.00139>
- [4] H. Abrougui, S. Nejjim, H. Dallagi, Roll control of a Tail-Sitter VTOL UAV, Int. J. Control. Energy . Electr. Eng., (CEEE). 7 (2019) 22-27.
- [5] B. Li, W. Zhou, J. Sun, C. Y. Wen, C. K. Chen, Development of model predictive controller for a Tail-Sitter VTOL UAV in hover flight, Sens., 18 (2018) 2859-2879. <https://doi.org/10.3390/s18092859>
- [6] J. A. Guerrero, R. Lozano, G. Romero, D. Lara, K. C. Wong, Robust control design based on sliding mode control for hover flight of a mini tail-sitter unmanned aerial vehicle, Annual. Conf. Indust. Electr., (2009) 2342–2347. <https://doi.10.1109/IECON.2009.5415267>
- [7] X. Lyu, J. Zhou, H. Gu, Z. Li, S. Shen, F. Zhang, Disturbance Observer Based Hovering Control of Quadrotor Tail-Sitter VTOL UAVs Using H_∞ Synthesis, IEEE. Robot. Autom. Lett., 3 (2018) 2910-2917. <https://doi.org/10.1109/LRA.2018.2847405>
- [8] Y. Yang, J. Zhu, X. Zhang, X. Wang, Active Disturbance Rejection Control of a Flying-Wing Tail Sitter in Hover Flight, IEEE/RSJ . Int. Conf. Intell. Robots. Syst., (2018) 6390-6396. <https://doi.10.1109/IROS.2018.8594470>
- [9] Z. Li, L. Zhang, H. Liu, Z. Zuo, C. Liu, Nonlinear robust control of tail-sitter aircrafts in flight mode transitions, Aerosp. Sci Technol., 81 (2018) 348-361. <https://doi.org/10.1016/j.ast.2018.08.021>
- [10] S.J. Cheng, H_∞ Control Sliding Mode Control of Magnetic Levitation System, Asian. J. Control., 4 (2002) 333-340. <https://doi.org/10.1111/j.1934-6093.2002.tb00361.x>
- [11] G. Suganya, J. Amla, S. P. Dwarakesh, Model Reference Adaptive Controller using MOPSO for a Nonlinear Boiler Turbine, Int. j. soft. comput. Eng., 4 (2014) 87-91.
- [12] P. Apkarian , D. Noll, The H_∞ control problem is solved, Aeros. Lab, Alain App., (2017)1-11. <https://doi.org/10.12762/2017.AL13-01>
- [13] A. Hatamlou, Black hole: A new heuristic optimization approach for data clustering, Inf. Sci ., 222 (2013) 175–184. <https://doi.org/10.1016/j.ins.2012.08.023>
- [14] H. I. Ali , M. A. Hadi, Optimal Nonlinear Controller Design for Different Classes of Nonlinear Systems Using Black Hole Optimization Method, Arab. J. Sci. Eng., 45 (2020) 7033-7053. <https://doi.org/10.1007/s13369-020-04650-z>
- [15] B. L. Stevens, F. L. Lewis, E. N. Johnson, Aircraft control and simulation: dynamics, controls design, and autonomous systems, 3rd ed, John Wiley . Sons, USA, 2015.
- [16] P. C. Garcia, R. Lozano, A. E. Dzul, Modelling and control of mini-flying machines, Spr. Sci. Business Media, London, 2006.
- [17] H. I. Ali, Swarm Intelligence to Robust Control Design, United Scholars Publications, USA, 2018.
- [18] Z. Kemin , D. Jhon, Essentials of Robust Control, Upper Saddle River, New Jersey: Prentice Hall Inc., 1998.
- [19] B. N. Hussein, N. Sulaiman, R. Kamil, M. H. Marhaban, H. I. Ali, H_∞ controller design to control the single axis magnetic levitation system with parametric uncertainty, J. Appl. Sci., 11(2011) 66-75. <https://doi.org/10.3923/jas.2011.66.75>
- [20] H. K. Khalil, Nonlinear Systems, 3rd ed, Upper Saddle River, New Jersey: Prentice Hall Inc., 2002.
- [21] A. A. Aly, Model Reference PID Control of an Electro-Hydraulic Drive, Int. J. Intell. Syst. Appl., 4 (2012) 2074-9058. <https://doi.org/10.5815/ijisa.2012.11.03>
- [22] H. I. Ali, H_∞ model reference controller design for magnetic levitation system, Eng. Technol. J. Eng., 36 (2018) 17–26. <https://doi.org/10.30684/etj.36.1A.3>
- [23] H. I. Ali, H. M. Jassim, A. F. Hasan, Optimal Nonlinear Model Reference Controller Design for Ball and Plate System, Arab. J. Sci. Eng., 44 (2019) 6757-6768. <https://doi.org/10.1007/s13369-018-3616-1>
- [24] E. Lavretsky K. A. Wise, Robust and adaptive control with aerospace applications, Springer, London, 2013.